Histochem Cell Biol (2011) 136:25–35
DOI 10.1007/s00418-011-0827-x

ORIGINAL PAPER

Immunolocalization of WNK4 in mouse kidney

Mayuko Ohno · Keiko Uchida · Teiko Ohashi · Kosaku Nitta · Akihito Ohta · Motoko Chiga · Sei Sasaki · Shinichi Uchida

Accepted: 24 May 2011 / Published online: 10 June 2011

Abstract Initial reports claim that WNK4 localization is mainly at intercellular junctions of distal convoluted tubules (DCT) and cortical collecting ducts (CCD) in the kidney. However, we recently clarified the major targets of WNK4 kinase to be the OSR1/SPAK kinases and the Na–Cl co-transporter (NCC), an apical membrane protein in the DCT, thus raising the question of whether the cellular localization of WNK4 is at intercellular junctions. In this study, we re-evaluate the intrarenal and intracellular immunolocalization of WNK4 in the mouse kidney using a newly generated anti-WNK4 antibody. By performing double immunofluorescence of WNK4 with several nephron-segment-specific markers, we have found that WNK4 is present in podocytes in glomeruli, the cortical thick ascending limb of Henle's loop including macula densa, and the medullary collecting ducts (MCD), in addition to the previously identified nephron segments, i.e., DCT and CCD. These results are consistent with the finding that WNK4 constitutes a kinase cascade with OSR1/SPAK and NCC in the DCT, and highlights a novel role for WNK4 in nephron segments newly identified as being WNK4-positive in this study.

Electronic supplementary material The online version of this article (doi:10.1007/s00418-011-0827-x) contains supplementary material, which is available to authorized users.

M. Ohno · K. Uchida (✉) · T. Ohashi · K. Nitta
Department of Medicine, Kidney Center,
Tokyo Women's Medical University,
8-1 Kawada-cho Shinjyuku-ku,
Tokyo 162-8666, Japan
e-mail: kuchida@kc.twmu.ac.jp

A. Ohta · M. Chiga · S. Sasaki · S. Uchida
Department of Nephrology, Tokyo Medical and Dental University, 1-5-45 Yushima Bunkyo, Tokyo 113-8519, Japan

Keywords WNK kinase · Na–Cl co-transporter · AQP2 water channel · Immunofluorescence · Immunoelectron microscopy

Introduction

Pseudohypoaldosteronism type II (PHAII) is an autosomal-dominant disorder characterized by hyperkalemia, acidosis, and hypertension (Gordon 1986). Wilson et al. identified the genes responsible for PHAII as being the With-No-Lysine kinase (*WNK*) 1 and *WNK4* genes (Wilson et al. 2001). Studies of monogenetic hypertensive diseases such as Liddle syndrome have provided insight into the mechanisms that underlie blood pressure regulation in the kidney (Schild et al. 1996). Similarly, the pathogenesis of PHAII recently identified by our group using *Wnk4*^{D561A} knockin mice revealed a novel signal transduction pathway in the kidney that regulates the thiazide-sensitive Na–Cl co-transporter (NCC) (Yang et al. 2007b). Recently, we also found that this novel signaling cascade from WNK4 to NCC (WNK4-OSR1/SPAK-NCC) is regulated by aldosterone in response to different amounts of NaCl intake (Chiga et al. 2008). Thus, the WNK4-OSR1/SPAK-NCC signaling cascade significantly contributes to the regulation of Na homeostasis in the kidney. In addition to NCC, many transporters and channels are reportedly regulated (mainly inhibited) by WNK4 in the *Xenopus* oocyte expression system (Jiang et al. 2007; Kahle et al. 2004b; Kahle et al. 2003; Yamauchi et al. 2004; Yang et al. 2003; Yang et al. 2007a). However, when analyzing *Wnk4*^{D561A} knockin mice, we found that the regulatory effects reported from those overexpression experiments were not necessarily observed in the kidney in vivo (Yang et al. 2007b). In our case, we reported that in Madin-Darby canine kidney cells

(MDCK), WNK4 localizes to intercellular junctions (Yamauchi et al. 2004), consistent with an initial report on WNK4 immunolocalization in the kidney (Wilson et al. 2001). We also found that the PHAII-causing mutant WNK4 increases paracellular chloride ion permeability in MDCK cells (Yamauchi et al. 2004). Another group later confirmed this finding (Kahle et al. 2004b). However, we were unable to detect increased chloride permeability in the distal nephron of *Wnk4*^{D561A} knockin mice. From this point of view, it was necessary to re-evaluate the intrarenal and intracellular localization of WNK4 in order to determine the physiological targets of WNK4 within the kidney. We recently succeeded at generating mice in which exon 7 of the *Wnk4* gene was deleted by gene targeting (Ohta et al. 2009). We generated a new antibody recognizing N-terminus of WNK4 in the same study and verified specificity to WNK4 using *Wnk4* gene-targeted mice (Ohta et al. 2009). In this study, we investigate the intrarenal immunolocalization of WNK4 in detail by using double immunofluorescence with several marker proteins for each nephron segment (Fushimi et al. 1993; Kaplan et al. 1996; Loffing et al. 2001). We report that WNK4 is not present at intercellular junctions, but is instead localized to the subapical cytosolic region in the distal convoluted tubules (Table 1).

Fig. 1 Immunoblots of WNK4. **a** Immunoblot of WNK4 of wild-type and hypomorphic mouse kidneys. *WT*: wild-type mice, *Hypo*: WNK4 hypomorphic mice. About 30 μg of whole lysates of kidney proteins (without nuclear fraction) was loaded in each lane. WNK4 hypomorphic mice express a shorter WNK4 protein lacking exons 7 and 8 (shown by an *arrow*). We occasionally got a relatively strong band (shown by an *asterisk*) around ~200 kD in addition to the true ~160-kD WNK4 band (shown by an *arrowhead*). However, the ~200-kD band could still be detected by the pre-absorbed antibody (4 μg/ml) with the antigen peptide (10 μg/ml), indicating that it is a non-specific signal. The three commercially available antibodies to WNK4 (×200 dilution) could not detect WNK4 protein in mouse kidney. **b** The effects of antibody absorption by the various concentrations of antigen peptide on the immunoblots of WNK4. One thousand times more peptide (0.1 vs. 100 μg/ml) could not block the non-specific band (shown by an *asterisk*). For immunoabsorption of the antibody, the diluted antibody (4 μg/ml) was incubated with the HPLC-purified antigen peptide for 2 h at 4°C before use. About 30 μg of whole lysates of kidney proteins (without nuclear fraction) was loaded in each lane. **c** Detection of mouse full length WNK4 overexpressed in COS7 cells. WNK4 antibody (4 μg/ml) detected a robust signal of WNK4 in COS7 cells transfected with mouse WNK4 expression vector, but not in cells transfected with an empty vector. A non-specific 200 kD band (shown by an *asterisk*) similar to that observed in mouse kidney was also observed in COS7 cells. Among the three commercially available antibodies to WNK4 (×200 dilution), only the one from Affinity Bioreagents could detect the overexpressed mouse WNK4 protein. About 2 μg of whole cell lysates was loaded in each lane. The antibodies from Novus and Alpha Diagnostics failed to detect the mouse WNK4 protein even when the loading amount was increased to 20 μg

Materials and methods

Immunofluorescent and immunoelectron microscopy

For immunofluorescence microscopy, kidneys were fixed by perfusion (through left ventricle) with paraformaldehyde (4%) in PBS. Tissue samples were soaked for several hours in 20% sucrose in PBS, embedded in Tissue Tek O.C.T. Compound (Sakura Finetechnical Co., Ltd, Tokyo, Japan), and snap frozen in liquid nitrogen. The primary antibodies used were: rabbit anti-WNK4 (×200 = 4 μg/ml) (Ohta et al. 2009), guinea pig anti-NCC (×200), and goat anti-AQP2 (×200) (Santa Cruz Biotechnology, Santa Cruz, CA), guinea pig anti-NKCC2 (×200) (Mutig et al. 2010) (Generous gift from S. Bachmann), mouse anti-parvalbumin (×10,000) (Swant, Bellinzona, Switzerland), mouse anti-calbindin-D28 K (×10,000) (Swant), guinea pig anti-nephrin (×200) (Acris, Heidelberg, Germany), mouse anti-occludin (×200) (Invitrogen, Carlsbad, CA), and mouse anti-ZO1 (×200) (Invitrogen, Carlsbad, CA). Alxa 488 or 546 dye-labeled (Invitrogen, Carlsbad, CA) secondary antibodies were used for immunofluorescence. Immunofluorescence images were obtained using the LSM510 Meta (Carl Zeiss). The anti-WNK4 antibody was generated using a KLH-conjugated HPLC-purified peptide (MLAPRNTETGVPMS + C) corresponding to the amino terminal portion of mouse WNK4 (Ohta et al. 2009). For double immunofluorescence with the rabbit anti-WNK4 antibody, a guinea pig anti-NCC antibody was generated using the same peptide sequence as antigen as has been

Table 1 Summary of immunolocalization of WNK4 in mouse kidney

	Gl (podocyte)	mTAL	cTAL	DCT1	DCT2	CNT	CCD	OMCD	IMCD
Marker	Nephrin	NKCC2	NKCC2	NCC, PV	NCC, CB	AQP2, CB	AQP2, CB	AQP2	AQP2
WNK4	++	–	+	+++	+++	++	++	++	++

Fluorescent signals were graded from – to +++

Gl glomerulus, *mTAL* medullary thick ascending limb of Henle's loop, *cTAL* cortical thick ascending limb of Henle's loop, *DCT* distal convoluted tubules, *CNT* connecting tubules, *CCD* cortical collecting ducts, *OMCD* outer medullary collecting ducts, *IMCD* inner medullary collecting ducts, *PV* parvalbumin, *CD* calbindin-D28 K

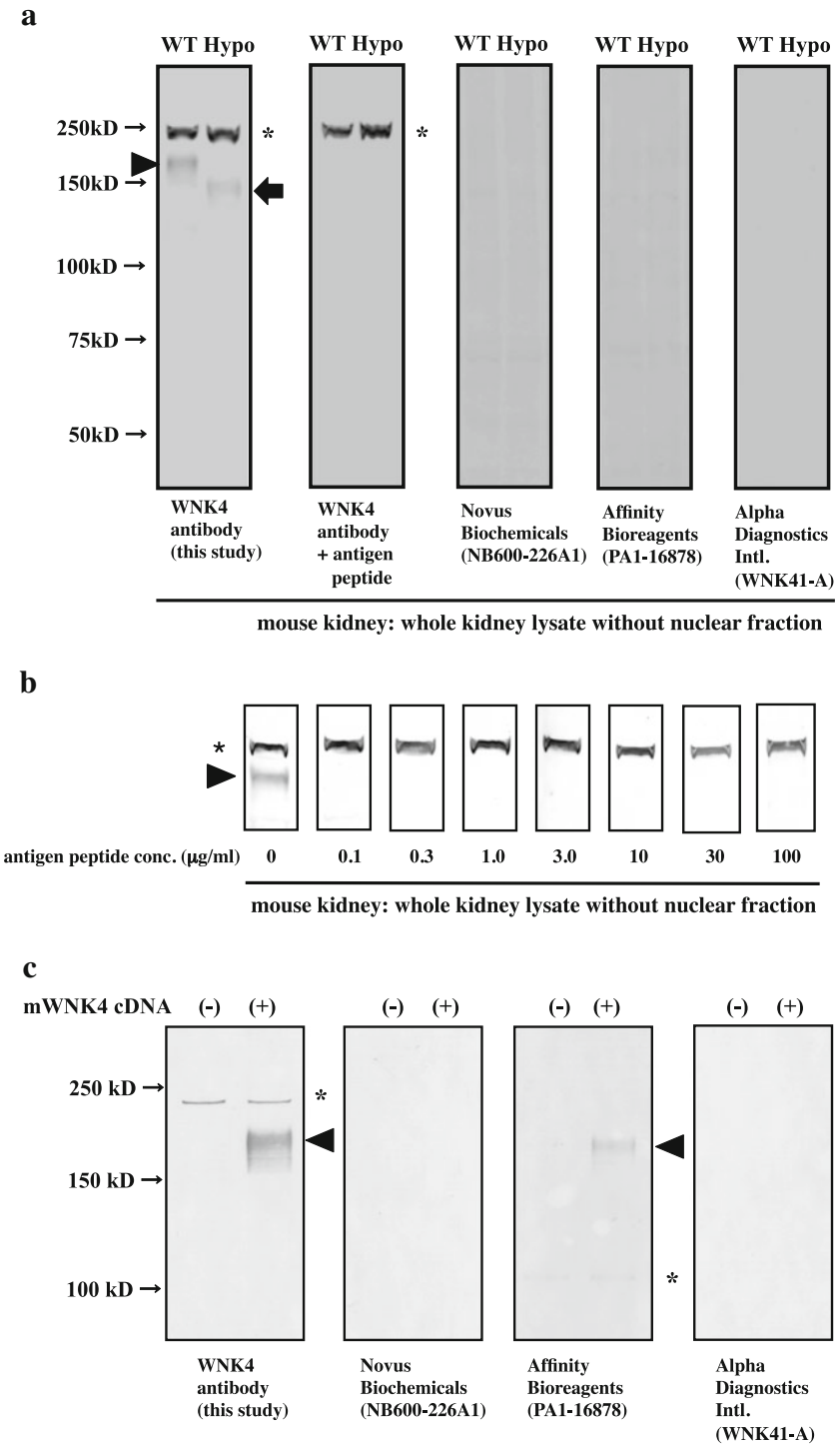

used for the commercially available rabbit anti-NCC (Chemicon, Billerica, MA). Double immunofluorescence using rabbit anti-NCC (Chemicon, Billerica, MA) and guinea pig anti-NCC antibodies showed that they completely co-localized (data not shown).

For immunoabsorption of the antibody for immunofluorescence, the diluted antibody was incubated with the HPLC-purified antigen peptide (10 μg/ml) for 2 h at 4°C before use.

Immunoblot

Whole kidney homogenate without nuclear fraction was used for immunoblot of WNK4. Two mouse kidneys were

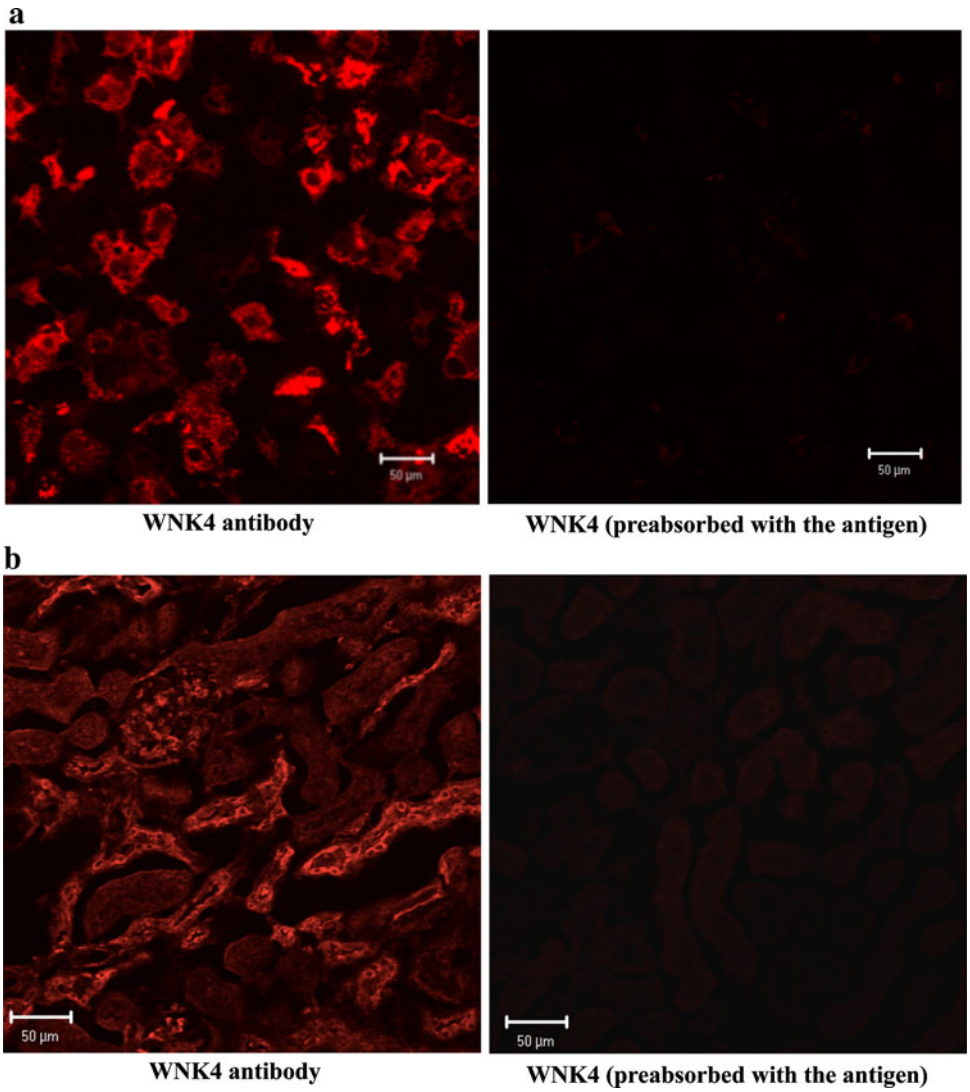

Fig. 2 The effect of antibody absorption on WNK4 immunofluorescence. **a** Immunofluorescence of WNK4 expressed in COS7 cells. COS7 cells transfected with mouse WNK4 cDNA were immunostained with the WNK4 antibody (4 μg/ml) (*left panel*) or the pre-absorbed WNK4 antibody (with 10 μg/ml antigen peptide) (*right panel*). Alxa-546 anti-rabbit IgG antibody was used for immunofluorescent detection. In the overexpression in COS7 cells, WNK4 was present in cytoplasm, some of them showing vesicular appearance (*left panel*). The pre-absorbed antibody failed to detect almost all signals as shown in the *left panel* (*right panel*). **b** Immunofluorescence of WNK4 in mouse kidney and its absorption by the antigen peptide. The immunofluorescent signals in mouse kidney (*left panel*) were also completely blocked by pre-incubation of the antibody (4 μg/ml) with the antigen peptide (10 μg/ml) (*right panel*)

homogenized in a homogenization buffer (1 ml) containing 0.25 M sucrose, 10 mM triethanolamine, 1 mM EGTA, 1 mM EDTA, 1 mM Na orthvanadate, 50 mM Na fluoride, cOmplete protease inhibitor cocktail (Roche, Indianapolis, IN), pH 7.5, and the homogenate was centrifuged at 600×*g* for 5 min to remove nuclear fraction. The supernatant was mixed with 2× SDS sample buffer (125 mM Tris–Cl, 4.3% SDS, 30% glycerol, 10% 2-mercaptoethanol, 0.1% bromophenol blue, pH 6.8), and then heated at 60°C for 20 min. About 30 μg of the protein sample was loaded in each lane of 7.5% SDS–PAGE. The signals were detected with alkaline phosphatase-conjugated secondary antibodies and Western Blue stabilized substrate for alkaline phosphatase (Promega, Madison, WI).

Transient expression of mouse WNK4 in COS7 cells

COS7 cells were transfected using Lipofectamine 2000 (Invitrogen, Carlsbad, CA) with mouse WNK4 cDNA in pCMV-SPORT6 expression vector (IMAGE clone ID 4234311, a generous gift from Alan S. L. Yu in University of Southern California Keck School of Medicine). Twenty hours after transfection, the cells were recovered in the same homogenization buffer as used for mouse kidney. For immunofluorescence, the transfected cells on cover slips were fixed with 4% paraformaldehyde in PBS for 15 min, and then permeabilized with 0.1% Triton X-100 in PBS for 10 min, before incubation with anti-WNK4 antibody (×200, at room temperature for 1 h). The signal was detected with Alxa 546 dye-labeled secondary antibody (Invitrogen, Carlsbad, CA).

Results

Specificity of anti-WNK4 antibody

The specificity of the anti-WNK4 antibody was previously verified by antibody absorption tests in immunofluorescence

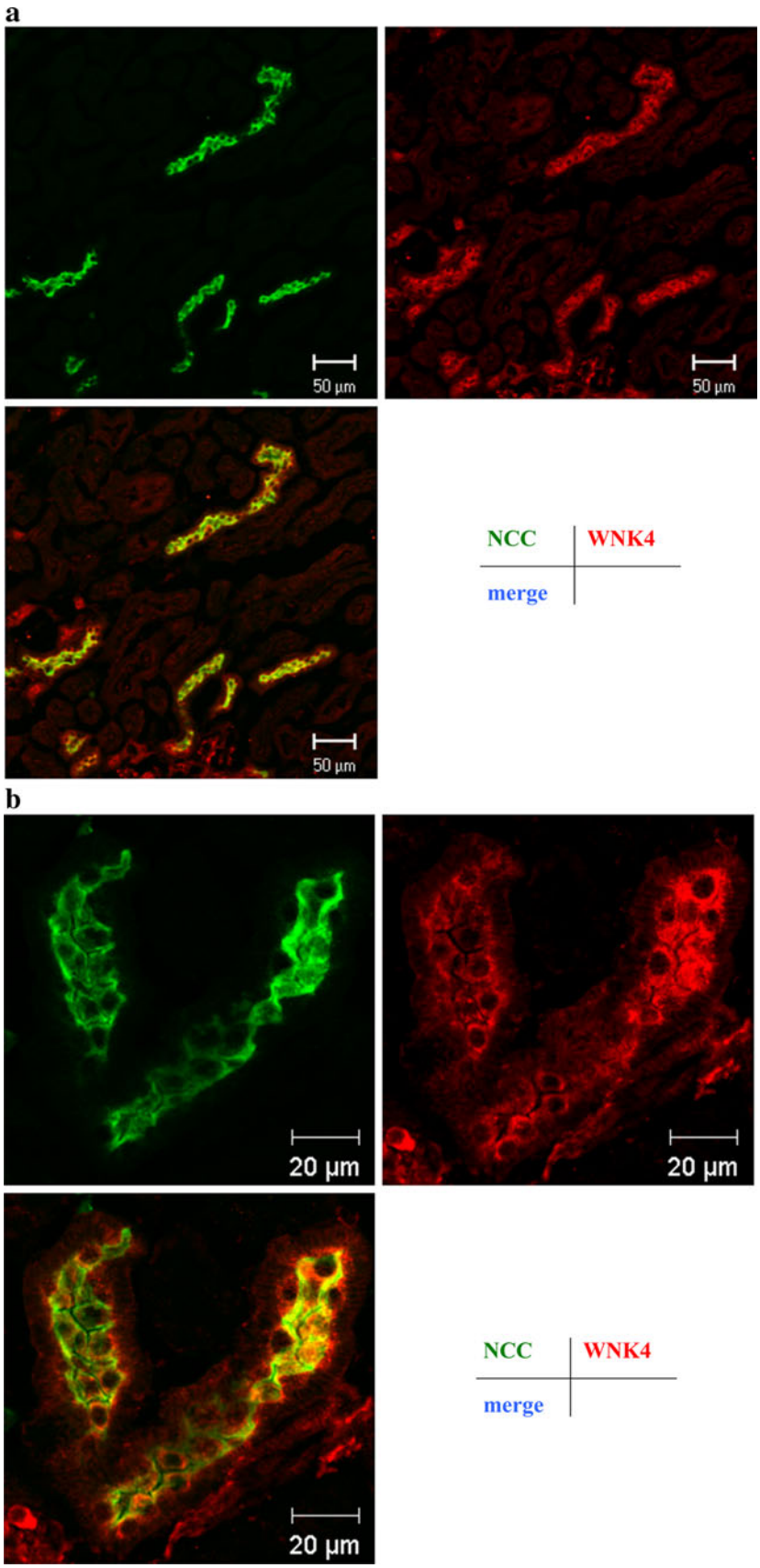

Fig. 3 **a** Double immunofluorescence of WNK4 in DCT. Double immunofluorescence of WNK4 and NCC. NCC is present in DCT1 and DCT2. All NCC-positive nephron are WNK4-positive. **b** Higher magnification of the DCT. NCC and WNK4 co-localize at subapical regions. **c** Double immunofluorescence of WNK4 with occludin and ZO1. DCT was identified by the strongest WNK4 signals in tubules and its morphological features including relatively high profile among distal nephron segments, abundant indentation of basal membranes, and subapical localization of nuclei. In the sections of DCT close to its transverse plane, the dot-like signals of occludin and ZO1 were detected (*arrows*). These *green signals* remains green after merge with red WNK4 signals, indicating that WNK4 is not co-localized with these tight junction proteins. There are some non-specific staining in the basal membranes of tubules by occludin and ZO1 antibodies. *Bar* 10 μm

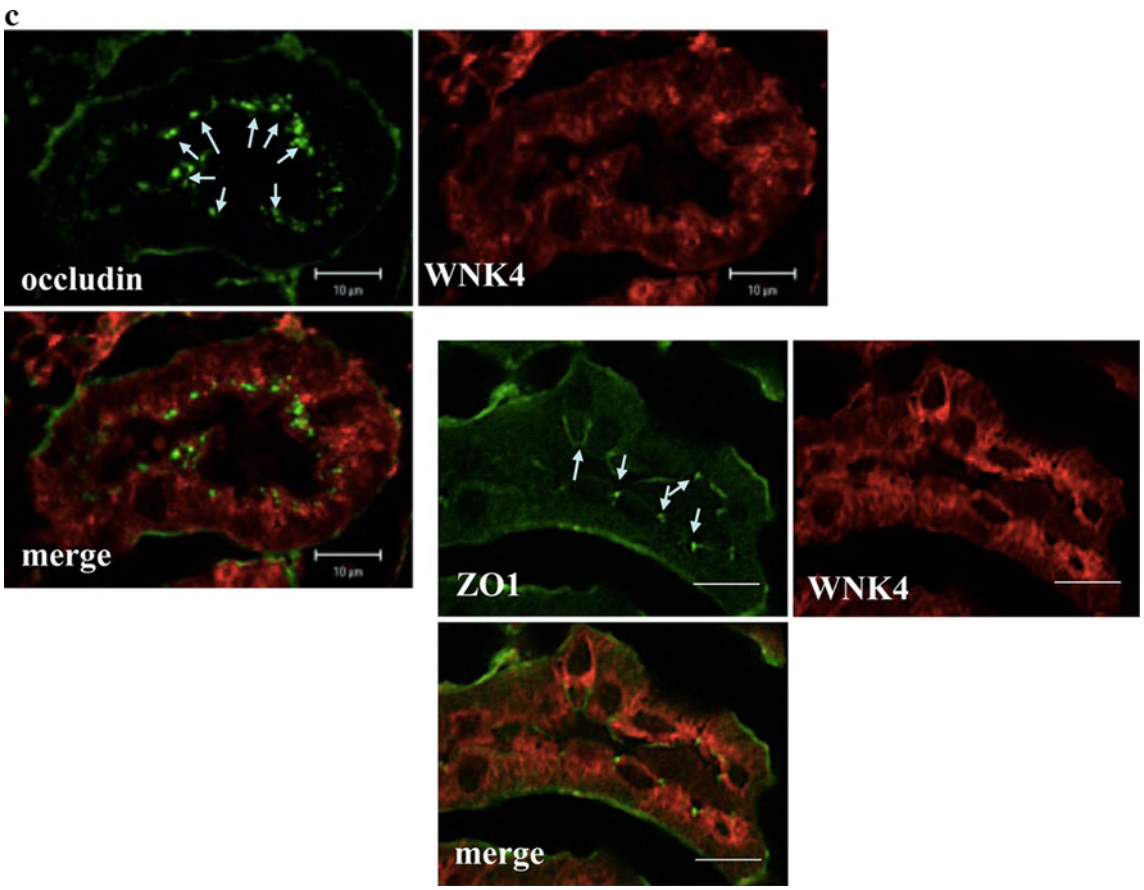

Fig. 3 continued

and immunoblotting using WNK4 hypomorphic mice (Ohta et al. 2009), and was further investigated in this study (Figs. 1, 2, and Supplementary Fig. 1). As we showed previously, the anti-WNK4 antibody could detect WNK4 protein (shown by an arrowhead) in wild-type mouse kidney and WNK4 lacking exons 7 and 8 (shown by an arrow) in WNK4 hypomorphic mouse kidney (Fig. 1a). Although these signals disappeared after the antibody (4 μg/ml) was pre-absorbed with the antigen peptide (10 μg/ml), we occasionally got a relatively strong band around ~200 kD in addition to the true ~160 kD WNK4 band. However, the ~200 kD band could still be detected by the pre-absorbed antibody with the higher concentration of antigen peptide (Fig. 1b). WNK4 signal could also be blocked with further lower concentrations of the peptide (Fig. 1b), indicating that the ~200 kD band is not an aggregate of WNK4 protein but a non-specific signal. Intensity of the non-specific band significantly decreased when whole kidneys were homogenized in a buffer containing detergents (1% NP40, 0.5% Na deoxycholate, 0.1% SDS in PBS), although WNK4 signal was also decreased (Supplementary Fig. 1). The reason for this phenomenon is not clear at present.

Specificity of the antibody was further verified by using overexpressed mouse WNK4 protein in COS7 cells. As shown in Fig. 1c, WNK4 antibody used in this study could detect a robust 160 kD signal only in the protein samples expressing mouse WNK4 cDNA. A ~200 kD non-specific band was also detected in COS7 cells. Among the three commercially available anti-WNK4 antibodies, only the one from Affinity Bioreagents could detect the overexpressed mouse WNK4 protein. However, the sensitivity was much lower than that of our antibody, consistent with the lack of signal in mouse kidney (Fig. 1a).

The specificity of signals in immunofluorescence was also verified by using the pre-absorbed antibody (Fig. 2). Mouse WNK4 immunofluorescence in COS7 cells was shown to be blocked by the pre-incubation of the antibody with the antigen peptide (10 μg/ml) (Fig. 2a). Similarly, the signals in immunofluorescence (Fig. 2b) in mouse kidney was blocked by the pre-incubation with the peptide, confirming that the signals are WNK4-specific.

Immunofluorescence of WNK4 in the mouse kidney

In Fig. 3a, NCC co-localizes with WNK4 in the kidney. All the NCC-positive tubules are WNK4-positive. At a higher

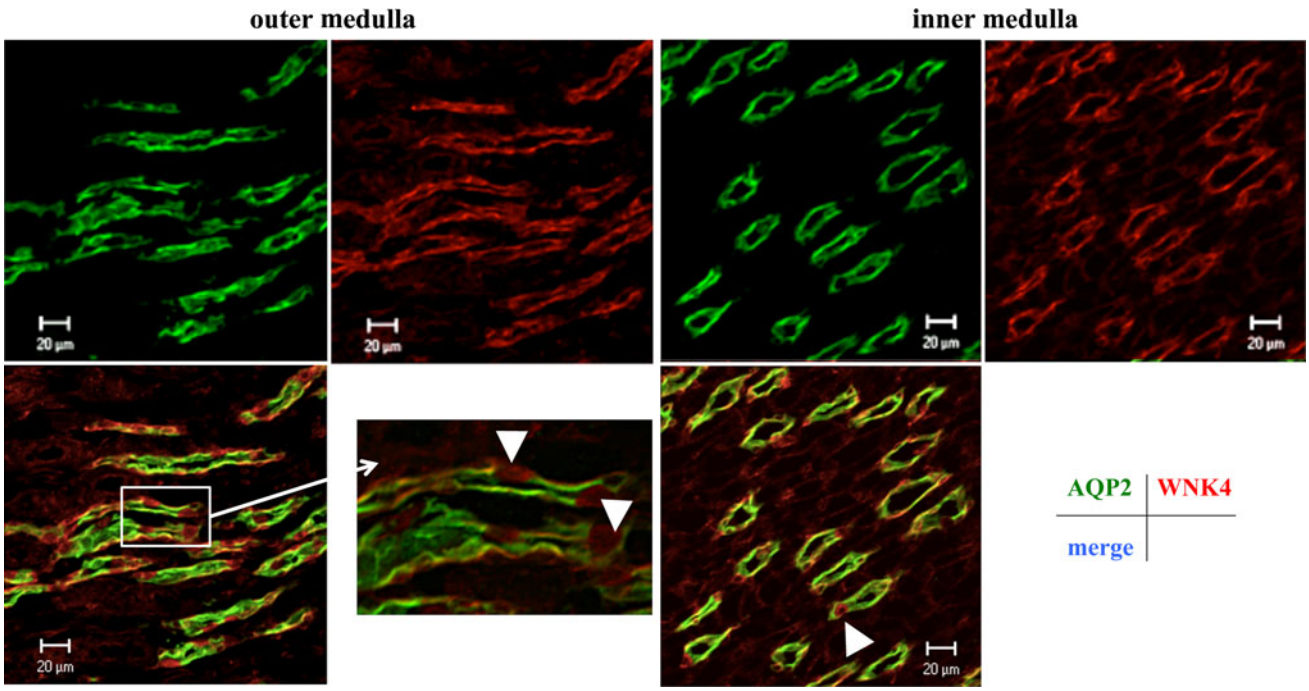

Fig. 4 Double immunofluorescence of WNK4 and AQP2. *Upper panels*: outer medullary AQP2-positive collecting ducts are WNK4-positive. AQP2-negative cells are also WNK4-positive (*arrowheads* in inset). *Lower panels*: inner medullary collecting ducts are WNK4-positive. AQP2-negative cells (*arrowhead*) are also WNK4-positive

magnification (Fig. 3b), WNK4 is present in the cytoplasm of the subapical region. Since WNK4 staining at intracellular junctions was previously reported (Wilson et al. 2001), we performed the double immunofluorescence of WNK4 with occludin and ZO1. Unlike the previous report, co-localization of WNK4 with these tight junction proteins is not observed in DCT (Fig. 1c) and in cortical nephron segments more distal to DCT (Supplementary Fig. 2). To further determine the WNK4 signal in the tubules other than the NCC-positive segment, double immunofluorescence with parvalbumin, calbindin-D28 K and AQP2 (Fushimi et al. 1993) was performed. As shown in Supplementary Fig. 3, all of the parvalbumin-positive tubules, which are DCT1 (Loffing et al. 2001), are WNK4-positive. As shown in the upper panels of Supplementary Fig. 4, most of the WNK4 signal co-localizes with calbindin28 K, which is present in DCT2, CNT, and CCD (Loffing et al. 2001). In the calbindin-D28 K-negative intercalated cells of CCD, WNK4 immunofluorescence is also weakly positive (Supplementary Fig. 4, lower panels). In the medullary and papillary collecting ducts, WNK4 immunofluorescence is also observed in AQP2-negative cells (Fig. 4, inset). In the principal cells of CCD, WNK4 immunofluorescence showed broad cytoplasmic staining (Fig. 4).

We next investigated WNK4 localization in the thick ascending limb of Henle's loop (TAL) by double immunofluorescence with NKCC2 (Kaplan et al. 1996). As shown in Fig. 5a, NKCC2 immunofluorescence in the medulla does not co-localize with WNK4, clearly indicating that WNK4 is not present in medullary TAL (mTAL). However, in cortical TAL (cTAL), NKCC2 immunofluorescence does co-localize with WNK4 (Fig. 5b, left panel). Macula densa is also WNK4-positive, although the signal was much weaker than that in cTAL (Fig. 5b, right panels).

As shown in Fig. 5b, WNK4 immunofluorescence is also observed in the glomeruli. Higher magnification of glomeruli (Fig. 6) showed a strong WNK4 signal, which is mostly co-localized with nephrin, suggesting that the main site of WNK4 expression in glomeruli is podocytes.

Discussion

We report here detailed intrarenal and cellular immunolocalization of WNK4 in mouse kidney. To understand the physiological role of WNK kinases in the kidney in vivo, information on the intrarenal localization of the WNK kinases is very important for determining the channels and transporters that are regulated by these kinases. The first report on the immunolocalization of WNK4 in the kidney by Wilson et al. describes WNK4 as being present in the intercellular junctions of the DCT and in the cytoplasm of the CCD (Wilson et al. 2001). The antibody used in that study was raised against human WNK4, but was used for staining mouse kidney. In fact, the authors detected a single band in an immunoblot of the kidney. However, the amino

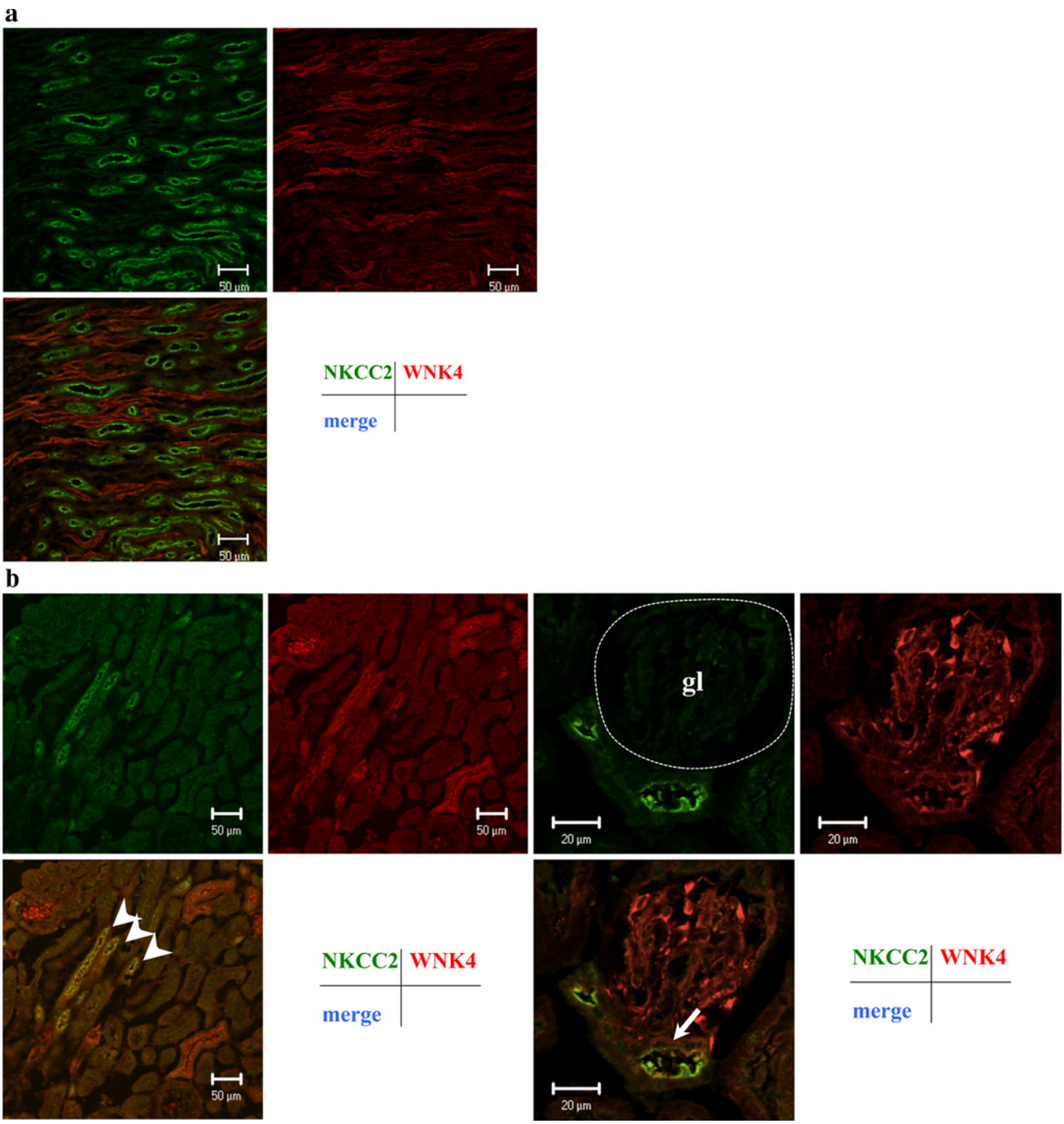

Fig. 5 Double immunofluorescence of WNK4 and NKCC2. **a** WNK4 is not present in medullary TAL. All NKCC2-positive nephrons in the outer medulla (medullary TAL) are WNK4-negative. **b** WNK4 is present in cortical TAL and macula densa. NKCC2-positive cortical tubules (cortical TAL) are WNK4-positive (shown in *yellow* by co-localization in the *left lower panel*, *arrowheads*). *Right panels*: Macula densa (*arrow*) adjacent to glomerulus (gl) is also weakly WNK4-positive. The signal in macula densa is weaker than that in CTAL. WNK4-positive cells are observed in the glomerulus

acid identity between human and mouse WNK4 within the region selected as the antigen peptide was less than 60%. The same group later reported that WNK4 localized to the extrarenal region by using a commercially available anti-WNK4 antibody (Novus Biologicals, Littleton. CO) (Kahle et al. 2004a). The authors described that WNK4 is also present in the intercellular junction in Cl transporting epithelia other than in kidney tubules (Kahle et al. 2004a). However, the specificity of the Novus anti-WNK4 antibody has not been well characterized. We have previously used

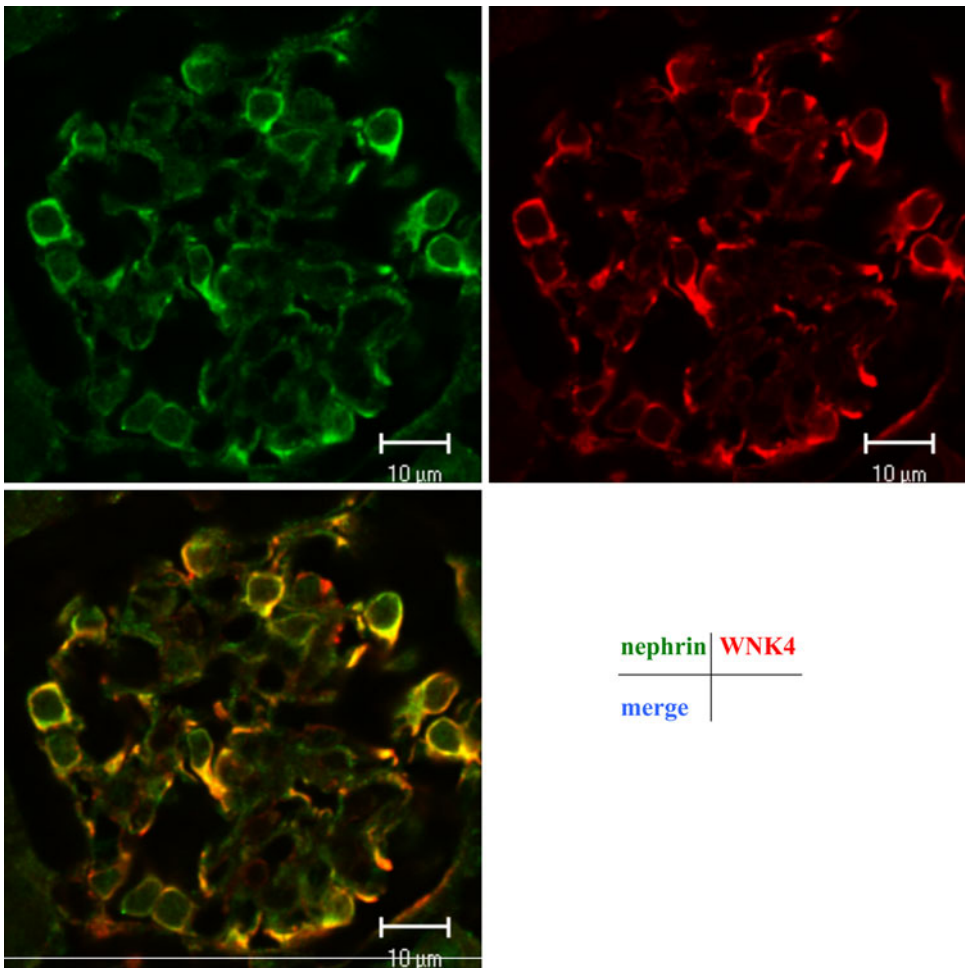

Fig. 6 Double immunofluorescence of WNK4 and nephrin. WNK4 signals in *red* are mostly co-localized with *green* nephrin signals, suggesting that WNK4 is mainly present in podocytes in glomeruli

another commercially available anti-WNK4 antibody (Alpha Diagnostics, San Antonio, TX) in our WNK4 D561A knockin mice (Yang et al. 2007b). The staining in the DCT was similar to the findings of Wilson et al., but was different to what we have found in this study. Both antibodies failed to detect overexpressed mouse WNK4 protein in the immunoblot of this study (Fig. 1c), raising a concern about the cellular localization of WNK4 determined by these antibodies.

Previous in situ hybridization studies of WNK4 in the kidney have been helpful for verifying the data obtained by immunostaining. WNK4 signals by in situ hybridization have been observed more broadly along the distal nephron compared to kidney-specific WNK1 in the DCT and CNT, namely in the thick ascending limb of Henle's loop (TAL) including macula densa, DCT, CNT, and collecting ducts (Delaloy et al. 2008; O'Reilly et al. 2006; O'Reilly et al. 2003). This is similar to that observed in this study, except for the absence of WNK4 immunofluorescence in mTAL. Although the reason for this discrepancy is not clear, the existence of a transcript does not necessarily mean the existence of its translational product. The lack of WNK4 protein in mTAL is consistent with our observation that increased phosphorylation of NKCC2 is not observed in our WNK4 knockin mice (manuscript in preparation). Since SPAK was shown to be present in mTAL (Rafiqi et al. 2010), and to phosphorylate NKCC2 (Reiche et al. 2010), phosphorylation of NKCC2 should have been increased in WNK4 knockin mice if WNK4 was present in mTAL. Furthermore, PHAII is sensitive to thiazide, not to furosemide; i.e., activation of furosemide-sensitive NKCC2 is not observed in PHAII patients.

In regard to WNK4's intracellular localization, WNK4 signal was observed in the subapical cytoplasm in the DCT (Fig. 3b). We could not observe apparent co-localization of WNK4 with ZO1 and occluding (Fig. 3c). This subapical localization of WNK4 in the DCT may be consistent with the notion of a functional interaction between WNK4 and NCC that we discovered in our WNK4 knockin mice. In collecting ducts, the signals were observed more broadly in cytoplasm. Again, WNK4 was not co-localized with ZO1 (Supplementary Fig. 2). The preferential localization of WNK4 in the subapical regions in cTAL and DCT may simply be explained by the fact that abundant mitochondria

occupy the cytoplasm in the basolateral sides of cTAL and DCT (Kriz and Kaissling 1985).

The role of WNK4 in the collecting ducts is currently unknown. It has been reported that the epithelial sodium channel (ENaC) and the ROMK potassium channel are regulated by WNK4 in *Xenopus* oocytes (Kahle et al. 2003; Ring et al. 2007a; Ring et al. 2007b). However, in our WNK4 knockin and hypomorphic mouse studies, data identifying these channels as direct targets of WNK4 were sought and not found.

We did observe positive staining with our anti-WNK4 antibody in the glomeruli, which was confirmed by double immunofluorescence with nephrin-showing WNK4 in the cytoplasm of podocytes. Previous in situ hybridization studies did not detect WNK4 mRNA in glomeruli. The reason for this discrepancy is not clear at present, although we could detect WNK4 mRNA by RT–PCR (Supplementary Fig. 5). In our WNK4 hypomorphic mice, however, albuminuria was not observed (unpublished observation). In order to determine the physiological role of WNK4 in these kidney cells other than DCT, generation of kidney-specific WNK4-null mice is necessary.

Finally, we have to mention a possible limitation of this study. Although we have extensively verified the specificity of our antibody to WNK4, all the results obtained in this study relies only on the single polyclonal antibody raised by a synthetic peptide. Since the immunolocalization of mouse WNK4 clarified in this study is not consistent with the previous report (Wilson et al. 2001), further attempt to generate another antibody to WNK4 will be necessary to confirm our findings.

In summary, we have clarified the intrarenal and intracellular immunolocalization of WNK4 in mouse kidney.

References

Chiga M, Rai T, Yang SS, Ohta A, Takizawa T, Sasaki S, Uchida S (2008) Dietary salt regulates the phosphorylation of OSR1/SPAK kinases and the sodium chloride cotransporter through aldosterone. Kidney Int 74:1403–1409

Delaloy C, Elvira-Matelot E, Clemessy M, Zhou XO, Imbert-Teboul M, Houot AM, Jeunemaitre X, Hadchouel J (2008) Deletion of WNK1 first intron results in misregulation of both isoforms in renal and extrarenal tissues. Hypertension 52:1149–1154

Fushimi K, Uchida S, Hara Y, Hirata Y, Marumo F, Sasaki S (1993) Cloning and expression of apical membrane water channel of rat kidney collecting tubule. Nature 361:549–552

Gordon RD (1986) Syndrome of hypertension and hyperkalemia with normal glomerular filtration rate. Hypertension 8:93–102

Jiang Y, Ferguson WB, Peng JB (2007) WNK4 enhances TRPV5-mediated calcium transport: potential role in hypercalciuria of familial hyperkalemic hypertension caused by gene mutation of WNK4. Am J Physiol Renal Physiol 292:F545–F554

Kahle KT, Wilson FH, Leng Q, Lalioti MD, O'Connell AD, Dong K, Rapson AK, MacGregor GG, Giebisch G, Hebert SC, Lifton RP (2003) WNK4 regulates the balance between renal NaCl reabsorption and K+ secretion. Nat Genet 35:372–376

Kahle KT, Gimenez I, Hassan H, Wilson FH, Wong RD, Forbush B, Aronson PS, Lifton RP (2004a) WNK4 regulates apical and basolateral Cl- flux in extrarenal epithelia. Proc Natl Acad Sci USA 101:2064–2069

Kahle KT, Macgregor GG, Wilson FH, Van Hoek AN, Brown D, Ardito T, Kashgarian M, Giebisch G, Hebert SC, Boulpaep EL, Lifton RP (2004b) Paracellular Cl- permeability is regulated by WNK4 kinase: insight into normal physiology and hypertension. Proc Natl Acad Sci USA 101:14877–14882

Kaplan MR, Plotkin MD, Lee WS, Xu ZC, Lytton J, Hebert SC (1996) Apical localization of the Na-K-Cl cotransporter, rBSC1, on rat thick ascending limbs. Kidney Int 49:40–47

Kriz W, Kaissling B (1985) Structural organization of the mammalian kidney. In: Seldin DW, Giebish G (eds) The Kidney: physiology and pathophysiology, vol 1. Raven Press, New York, pp 265–306

Loffing J, Loffing-Cueni D, Valderrabano V, Klausli L, Hebert SC, Rossier BC, Hoenderop JG, Bindels RJ, Kaissling B (2001) Distribution of transcellular calcium and sodium transport pathways along mouse distal nephron. Am J Physiol Renal Physiol 281:F1021–F1027

Mutig K, Saritas T, Uchida S, Kahl T, Borowski T, Paliege A, Bohlick A, Bleich M, Shan Q, Bachmann S (2010) Short-term stimulation of the thiazide-sensitive Na+-Cl- cotransporter by vasopressin involves phosphorylation and membrane translocation. Am J Physiol Renal Physiol 298:F502–F509

Ohta A, Rai T, Yui N, Chiga M, Yang SS, Lin SH, Sohara E, Sasaki S, Uchida S (2009) Targeted disruption of the Wnk4 gene decreases phosphorylation of Na-Cl cotransporter, increases Na excretion and lowers blood pressure. Hum Mol Genet 18:3978–3986

O'Reilly M, Marshall E, Speirs HJ, Brown RW (2003) WNK1, a gene within a novel blood pressure control pathway, tissue-specifically generates radically different isoforms with and without a kinase domain. J Am Soc Nephrol 14:2447–2456

O'Reilly M, Marshall E, Macgillivray T, Mittal M, Xue W, Kenyon CJ, Brown RW (2006) Dietary electrolyte-driven responses in the renal WNK kinase pathway in vivo. J Am Soc Nephrol 17:2402–2413

Rafiqi FH, Zuber AM, Glover M, Richardson C, Fleming S, Jovanovic S, Jovanovic A, O'Shaughnessy KM, Alessi DR (2010) Role of the WNK-activated SPAK kinase in regulating blood pressure. EMBO Mol Med 2:63–75

Reiche J, Theilig F, Rafiqi FH, Carlo AS, Militz D, Mutig K, Todiras M, Christensen EI, Ellison DH, Bader M, Nykjaer A, Bachmann S, Alessi D, Willnow TE (2010) SORLA/SORL1 functionally interacts with SPAK to control renal activation of Na(+)-K(+)-Cl(-) cotransporter 2. Mol Cell Biol 30:3027–3037

Ring AM, Cheng SX, Leng Q, Kahle KT, Rinehart J, Lalioti MD, Volkman HM, Wilson FH, Hebert SC, Lifton RP (2007a) WNK4 regulates activity of the epithelial Na+ channel in vitro and in vivo. Proc Natl Acad Sci USA 104:4020–4024

Ring AM, Leng Q, Rinehart J, Wilson FH, Kahle KT, Hebert SC, Lifton RP (2007b) An SGK1 site in WNK4 regulates Na+ channel and K+ channel activity and has implications for aldosterone signaling and K+ homeostasis. Proc Natl Acad Sci USA 104:4025–4029

Schild L, Lu Y, Gautschi I, Schneeberger E, Lifton RP, Rossier BC (1996) Identification of a PY motif in the epithelial Na channel subunits as a target sequence for mutations causing channel activation found in Liddle syndrome. EMBO J 15:2381–2387

Wilson FH, Disse-Nicodeme S, Choate KA, Ishikawa K, Nelson-Williams C, Desitter I, Gunel M, Milford DV, Lipkin GW, Achard JM, Feely MP, Dussol B, Berland Y, Unwin RJ, Mayan

H, Simon DB, Farfel Z, Jeunemaitre X, Lifton RP (2001) Human hypertension caused by mutations in WNK kinases. Science 293:1107–1112

Yamauchi K, Rai T, Kobayashi K, Sohara E, Suzuki T, Itoh T, Suda S, Hayama A, Sasaki S, Uchida S (2004) Disease-causing mutant WNK4 increases paracellular chloride permeability and phosphorylates claudins. Proc Natl Acad Sci USA 101:4690–4694

Yang CL, Angell J, Mitchell R, Ellison DH (2003) WNK kinases regulate thiazide-sensitive Na-Cl cotransport. J Clin Invest 111:1039–1045

Yang CL, Liu X, Paliege A, Zhu X, Bachmann S, Dawson DC, Ellison DH (2007a) WNK1 and WNK4 modulate CFTR activity. Biochem Biophys Res Commun 353:535–540

Yang SS, Morimoto T, Rai T, Chiga M, Sohara E, Ohno M, Uchida K, Lin SH, Moriguchi T, Shibuya H, Kondo Y, Sasaki S, Uchida S (2007b) Molecular pathogenesis of pseudohypoaldosteronism type II: generation and analysis of a Wnk4(D561A/+) knockin mouse model. Cell Metab 5:331–344